World Journal of Innovation and Modern Technology, Vol. 7, Issue 6, (Dec) 2024
ISSN 2682-5910
DOI: 10.53469/wjimt.2024.07(06).16

Venturi Aeration Systems Design and Performance Evaluation in High Density Aquaculture

Kai Xu[1,*], Xiaoyue Xu[1], Hongxia Wu[1], Ruihong Sun[2]

[1]Wuhan Popularization Technology Co., Ltd.
[2]Taizhou Luyuan Plastic Industry Co., Ltd.
Correspondence Author, kai.a3a4@gmail.com

Abstract: ***The efficiency of Venturi-based aeration systems depends heavily on throat length and the number of air holes (NH), which influence key parameters such as oxygen transfer efficiency (KLa20), standard aeration efficiency (SAE), and bubble dynamics. This study examined the performance of Venturi devices with throat lengths of 20, 40, 60, 80, and 100 mm and NH configurations ranging from 5 to 20 under controlled aquaculture conditions. The results demonstrated that a throat length of 100 mm with NH=20 achieved the highest SAE of 1.28 kg O_2/kWh and produced the smallest bubble size of 0.03 mm. Bubble size decreased consistently with increasing NH, while longer throat lengths promoted uniform bubble distribution, enhancing gas-liquid mass transfer efficiency. A 3D analysis revealed that oxygen transfer efficiency plateaued beyond NH=15 due to turbulence saturation, highlighting the need for balanced design parameters. These findings provide practical design recommendations for optimizing Venturi aeration systems, particularly for high-density aquaculture, where efficient oxygenation and energy savings are critical. Future studies should investigate the effects of environmental variables and assess long-term system stability under real-world operational conditions.***

Keywords: Venturi aeration systems; Oxygen transfer efficiency; Standard aeration efficiency; Bubble dynamics; High-density aquaculture.

1. INTRODUCTION

The growing global demand for aquaculture has intensified the need for advanced oxygenation technologies to sustain aquatic life, particularly in high-density farming systems. Dissolved oxygen (DO) is a key determinant of the health and productivity of aquatic organisms, yet natural replenishment through photosynthesis and diffusion often proves inadequate. Artificial aeration systems have become indispensable for maintaining optimal DO levels in modern aquaculture, addressing both environmental and operational challenges.

Venturi-based aeration systems are widely recognized for their simplicity and efficiency in oxygen transfer. These systems utilize the Venturi effect, where air is entrained into water under negative pressure at the throat, creating micro- and nano-sized bubbles that enhance gas-liquid interaction. Extensive research has highlighted the influence of geometric parameters on the performance of Venturi devices. Issa et al. (2013) demonstrated that a throat length of 100 mm with 17 air holes achieved a peak standard aeration efficiency (SAE) of 1.25×10^{-2} kg O_2/kWh, emphasizing the importance of throat length and air hole configuration. Yadav et al. (2020) and Gu et al. (2020) and Luo et al. (2020) similarly reported that optimizing air hole placement along the throat significantly improves turbulence and oxygen dissolution efficiency. Park et al. (2017) further investigated nozzle angles and aeration depths, showing that these factors directly affect bubble generation and oxygen transfer rates. The role of flow dynamics in Venturi systems has also been extensively studied. Yang et al. (2022) highlighted how flow velocity and Reynolds number impact air entrainment rates, while Zhu et al. (2024) demonstrated that optimal throat geometry reduces asymmetry in water flow, enhancing bubble uniformity. These findings underscore the need for precise control of Venturi device design to maximize oxygen transfer efficiency. While geometric and fluid dynamic optimizations have been thoroughly explored, the material composition of Venturi devices remains underdeveloped. Traditional systems are predominantly constructed from metals, which are durable but prone to corrosion in saline environments and involve high manufacturing costs. Recent studies have explored the use of alternative materials such as plastics for engineering applications. Plastics offer corrosion resistance, reduced weight, and lower production costs, making them an attractive option for aquaculture systems (Lian et al., 2024; Liu et al., 2024). However, their application in Venturi-based aerators has not been comprehensively evaluated.

This study addresses this gap by developing a Venturi aeration system constructed from agricultural plastics. Computational fluid dynamics (CFD) simulations were employed to optimize the geometric design, focusing on

air hole configuration and bubble distribution. The system was experimentally evaluated to assess its performance in high-density aquaculture environments, with an emphasis on SAE, DO levels, and economic feasibility. The findings aim to provide practical and sustainable solutions for modern aquaculture while advancing the application of innovative materials in aeration technology.

2. MATERIALS AND METHODS

2.1 Fabrication of the Venturi Aeration Device

The Venturi aeration device was constructed using modular throat sections with lengths of 20 mm, 40 mm, 60 mm, 80 mm, and 100 mm. Each section was fabricated from agricultural-grade plastic to ensure corrosion resistance, lightweight construction, and operational stability in aquatic environments. The throat section, where air entrainment occurs, was designed with symmetrically distributed air holes (2 mm diameter) along its length. The number of air holes (NH) was varied between 5 and 20, depending on the throat length. This modular design allowed a systematic evaluation of the effects of throat length and NH on aeration efficiency. Computational fluid dynamics (CFD) simulations were used to optimize the design, ensuring uniform air distribution and efficient bubble formation.

2.2 Experimental Setup

The experiments were conducted in a closed-loop water circulation system to simulate aquaculture conditions, as illustrated in the schematic diagram. A 500 L water tank maintained at a constant temperature of 20°C was used as the test chamber. A centrifugal pump (1 h.p., 2,840 rpm) ensured a stable water flow rate of 0.5 m^3/min. The Venturi device was positioned in-line, with an air entrance located at the top of the throat section for atmospheric air entrainment. A pressure gauge and valve were installed upstream of the Venturi device to regulate water flow and pressure.

Dissolved oxygen (DO) levels were monitored using a calibrated DO meter (DO Meter) and probe (DO Probe) positioned at the outlet of the tank. Bubble behavior and distribution were observed visually in the water tank, with high-speed imaging used for detailed analysis. The schematic diagram outlines the water flow direction, air inlet, and key components used in the setup.

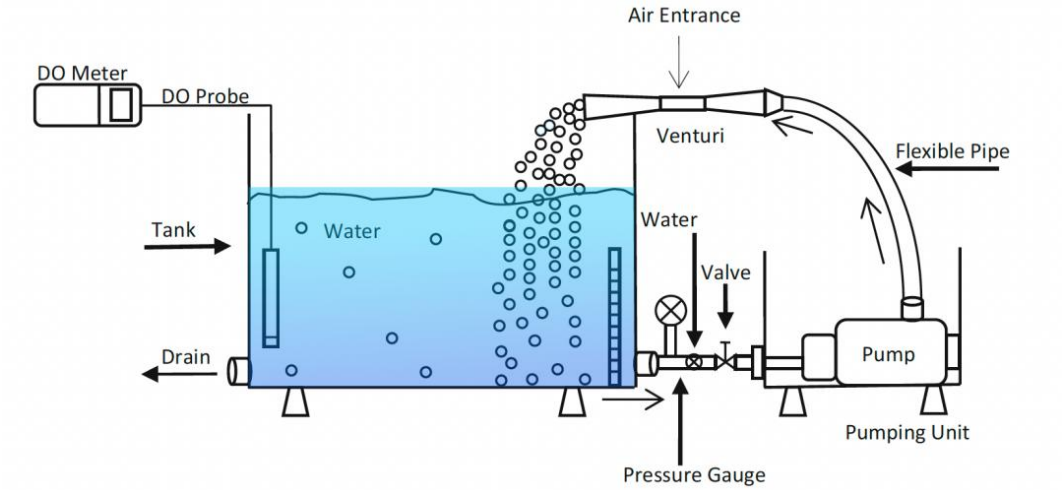

Figure 1: Experimental Setup for Venturi Aeration System

2.3 Experimental Procedure

Prior to each experiment, tap water was deoxygenated by adding 10 mg/L sodium sulfite with 0.1 mg/L cobalt chloride as a catalyst, ensuring initial DO levels below 1 mg/L. The pump circulated water through the Venturi device in a closed loop, and DO levels were recorded at 1-minute intervals using the DO meter until the water approached oxygen saturation. The valve was adjusted to maintain a stable water flow rate, while the pressure gauge monitored the system's operational pressure.

The Venturi aeration device was tested for throat lengths of 20, 40, 60, 80, and 100 mm, with air hole configurations ranging from 1 to 17 holes depending on the throat length. Each configuration was assessed for its impact on oxygen transfer efficiency, bubble generation, and energy consumption. Bubble size and distribution were recorded using high-speed imaging to evaluate the uniformity and efficiency of air entrainment.

2.4 Throat Section Variations

The experimental evaluation focused on varying the throat length and air hole number to determine their effects on aeration performance. For each throat length, air hole configurations were tested as follows:

- 20 mm throat: 1–5 air holes
- 40 mm throat: 1–7 air holes
- 60 mm throat: 1–9 air holes
- 80 mm throat: 1–13 air holes
- 100 mm throat: 1–17 air holes

These configurations were selected to systematically analyze the relationship between throat geometry and aeration performance, including bubble size, turbulence, and oxygen transfer efficiency.

2.5 Data Collection and Analysis

Oxygen transfer efficiency was quantified by calculating the oxygen transfer coefficient (KLa20) and standard aeration efficiency (SAE) (Li et al., 2022). The KLa20 was determined using the following formula:

$$KLa_T = \frac{\ln(C_s - C_0) - \ln(C_s - C_t)}{t} \quad (1)$$

Where Cs is the saturation DO concentration, C0 is the initial DO concentration, Ct is the DO concentration at time t, and t is the elapsed time. SAE was calculated using (Zhang et al., 2024):

$$SAE = \frac{SOTR}{P} \quad (2)$$

Where SOTR is the standard oxygen transfer rate (kgO_2/h), and P is the power input (kW). DO readings were recorded every minute until oxygen saturation was achieved. Each experimental condition was repeated three times, and the average values were reported with standard deviations. Polynomial regression models were used to analyze the relationship between the experimental variables and performance metrics, with coefficients of determination (R^2) used to evaluate model accuracy.

3. RESULTS AND DISCUSSION

3.1 Oxygen Transfer Coefficient (KLa20)

Figure 2a illustrates the relationship between KLa20 and the number of air holes (NH) for various throat lengths. Across all configurations, KLa20 increased with NH. The highest values recorded were 0.57 h^{-1}, 0.74 h^{-1}, 0.91 h^{-1}, 1.02 h^{-1}, and 1.072 h^{-1} for throat lengths of 20 mm, 40 mm, 60 mm, 80 mm, and 100 mm, respectively, at NH=17.5. These results align closely with the findings of Li et al. (2023) and Masarova et al. (2024), who demonstrated that longer throat lengths enhance turbulence intensity, resulting in improved oxygen dissolution. Similarly, Zhang et al. (2024) reported that an extended flow path in Venturi systems increases gas-liquid contact time, further promoting oxygen transfer. However, the diminishing rate of improvement observed beyond a throat length of 80 mm suggests a saturation effect, likely due to turbulence reaching its upper limit of effectiveness. This observation highlights the need to carefully balance throat length with system energy input for optimal performance.

3.2 Standard Aeration Efficiency (SAE)

The SAE values for throat lengths of 20 mm and 100 mm, presented in Figure 2b, demonstrate a clear dependence on NH. For the 100 mm throat length, SAE increased steadily with NH, reaching 1.28 kg O_2/kWh at NH=17.5, while the 20 mm throat length achieved a lower efficiency of 0.68 kgO_2/kWh under the same conditions. These results emphasize the energy efficiency benefits of longer throat lengths. However, a noticeable plateau in SAE was observed beyond NH=15, particularly for the 100 mm throat length. This trend may be attributed to excessive turbulence, which can reduce bubble retention time and limit oxygen transfer. Sun et al. (2024) similarly reported

that overly high air flow rates in Venturi systems can diminish efficiency due to bubble coalescence. These findings underscore the importance of optimizing NH to avoid unnecessary energy losses while maintaining high oxygen transfer rates.

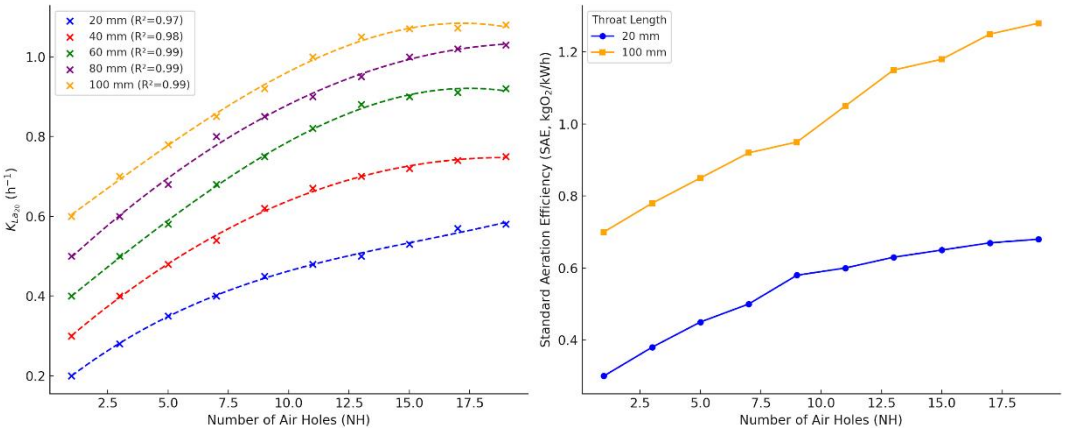

Figure 2: Extended Oxygen Transfer Coefficient and Energy Efficiency in Venturi Aeration Systems

3.3 Combined Effects of Throat Length and NH on Oxygen Efficiency

The combined influence of throat length and NH on oxygen efficiency is illustrated in the 3D surface plot in Figure 3a. Oxygen efficiency increased significantly with both parameters, peaking at 78% for a throat length of 100 mm and NH=20. For throat lengths shorter than 60 mm, efficiency remained below 74%, even at the highest NH values. This clearly highlights the critical role of longer throat lengths in achieving superior oxygen transfer performance. The plateau observed at NH values beyond 15 for throat lengths exceeding 80 mm reflects the limitations of turbulence-driven oxygen transfer. Similar observations were made by Liu et al. (2024), who noted that turbulence intensity contributes positively to oxygen transfer only up to a threshold, beyond which its effects become counterproductive due to bubble coalescence. These results provide further evidence of the need for a balanced system design to maximize efficiency without overloading the system.

3.4 Bubble Size and Uniformity

Figure 3b shows the relationship between bubble size and NH for various throat lengths. As NH increased, bubble size decreased consistently across all configurations. For the 100 mm throat length, bubble size was reduced to 0.03 mm at NH=20, reflecting the superior ability of longer throat lengths to generate smaller bubbles. Smaller bubbles not only improve gas-liquid mass transfer efficiency due to their larger surface area-to-volume ratio but also contribute to more uniform oxygen dissolution. These findings are supported by Xu et al. (2024) and Lin et al. (2024) and Cheng et al. (2024), who demonstrated that reduced bubble size significantly enhances oxygen transfer rates in aquaculture systems. Furthermore, Wang et al. (2024) and Ahad et al. (2023) conducted CFD simulations that corroborated these experimental results, showing that throat lengths exceeding 80 mm produce bubbles with consistent size and distribution, optimizing system performance.

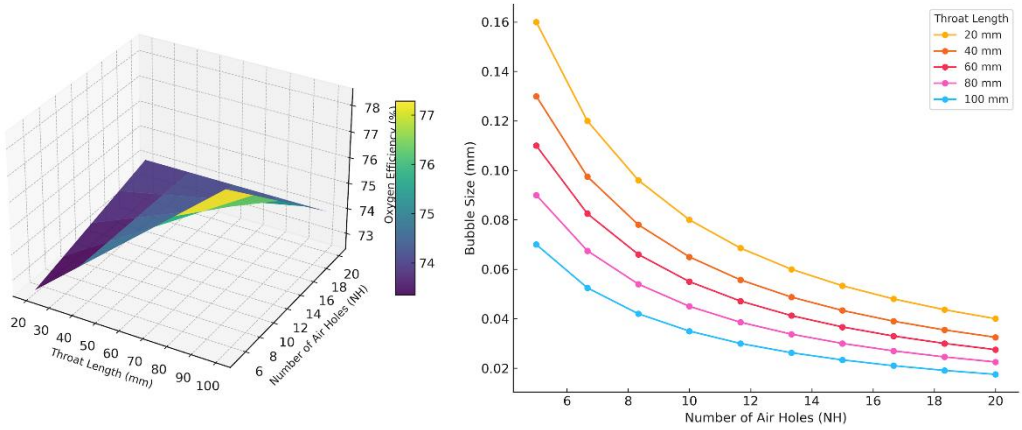

Figure 3: 3D Analysis of Oxygen Efficiency and Bubble Dynamics in Aeration Systems

3.5 Implications for Aeration System Design

The results of this study provide clear guidelines for optimizing Venturi-based aeration systems:

- Throat Length: Throat lengths of 80–100 mm deliver the best balance between oxygen transfer efficiency, energy consumption, and bubble size reduction. This range ensures sufficient turbulence intensity and gas-liquid contact time without causing excessive energy losses.

- Number of Air Holes (NH): NH values of 15–20 are recommended for achieving maximum performance. Beyond this range, further increases in NH yield diminishing returns in oxygen efficiency and SAE, as shown in Figures 2 and 3.

These findings align with practical design recommendations by Xia et al. (2024) and Wambua et al. (2020), who emphasized the importance of scalability and energy efficiency in designing systems for high-density aquaculture environments. By adopting these optimizations, Venturi systems can achieve both high oxygenation rates and cost-effective energy usage.

4. CONCLUSION

This study examined the effects of throat length and the number of air holes (NH) on the performance of Venturi-based aeration systems. The results show that throat lengths of 80–100 mm and NH values in the range of 15–20 deliver the best balance between oxygen transfer efficiency (KLa20), energy efficiency (SAE), and bubble size uniformity. Under these conditions, the 100 mm throat length achieved the highest SAE of 1.28 kg O_2/kWh and generated the smallest bubbles (0.03 mm) at NH=20. While increased turbulence and gas-liquid contact improved performance, the plateau observed in efficiency beyond NH=15 highlights the need for careful optimization to avoid diminishing returns. These findings provide actionable insights for designing efficient aeration systems for high-density aquaculture.

Further research should focus on understanding the impact of environmental variables such as water temperature, salinity, and flow velocity on system performance. Additional studies on the interplay between throat geometry, NH, and nozzle design will help refine operational parameters. Long-term evaluations of system stability and energy efficiency under real-world conditions are essential to ensure scalability and reliability. These efforts will pave the way for more sustainable and cost-effective aeration technologies.

REFERENCES

[1] Issa, H. M. (2013). Characterization and improvement of a surface aerator for water treatment (Doctoral dissertation, Institut National Polytechnique de Toulouse-INPT).
[2] Yadav, A., Kumar, A., & Sarkar, S. (2020). An experimental study to evaluate the efficacy of air entrainment holes on the throat of a venturi aeration system. Aquaculture International, 28, 1057-1068.
[3] Gu, J., Narayanan, V., Wang, G., Luo, D., Jain, H., Lu, K.,... & Yao, L. (2020, November). Inverse design tool for asymmetrical self-rising surfaces with color texture. In Proceedings of the 5th Annual ACM Symposium on Computational Fabrication (pp. 1-12).
[4] Luo, D., Gu, J., Qin, F., Wang, G., & Yao, L. (2020, October). E-seed: shape-changing interfaces that self drill. In Proceedings of the 33rd Annual ACM Symposium on User Interface Software and Technology (pp. 45-57).
[5] Park, S. K., & Yang, H. C. (2017). Experimental investigation on mixed jet and mass transfer characteristics of horizontal aeration process. International Journal of Heat and Mass Transfer, 113, 544-555.
[6] Yang, J., Chen, T., Qin, F., Lam, M. S., & Landay, J. A. (2022, April). Hybridtrak: Adding full-body tracking to vr using an off-the-shelf webcam. In Proceedings of the 2022 CHI Conference on Human Factors in Computing Systems (pp. 1-13).
[7] Zhu, J., Xu, T., Zhang, Y., & Fan, Z. (2024). Scalable Edge Computing Framework for Real-Time Data Processing in Fintech Applications. International Journal of Advance in Applied Science Research, 3, 85-92.
[8] Lian J. Research on Data Quality Analysis Based on Data Mining. Academic Journal of Science and Technology. 2024 Oct 10;12(3):16-9.
[9] Liu, Z., Costa, C., & Wu, Y. (2024). Data-Driven Optimization of Production Efficiency and Resilience in Global Supply Chains. Journal of Theory and Practice of Engineering Science, 4(08), 23-33.

[10] Liu, Z., Costa, C., & Wu, Y. (2024). Quantitative Assessment of Sustainable Supply Chain Practices Using Life Cycle and Economic Impact Analysis.
[11] Liu, Z., Costa, C., & Wu, Y. (2024). Leveraging Data-Driven Insights to Enhance Supplier Performance and Supply Chain Resilience.
[12] Li, W. (2022, April). Rural-to-Urban Migration and Overweight Status in Low-and Middle-Income Countries: Evidence From Longitudinal Data in Indonesia. In PAA 2022 Annual Meeting. PAA.
[13] Li, W. (2022). How Urban Life Exposure Shapes Risk Factors of Non-Communicable Diseases (NCDs): An Analysis of Older Rural-to-Urban Migrants in China. Population Research and Policy Review, 41(1), 363-385.
[14] Zhang, Y., & Fan, Z. (2024). Memory and Attention in Deep Learning. Academic Journal of Science and Technology, 10(2), 109-113.
[15] Zhang, Y., & Fan, Z. (2024). Research on Zero knowledge with machine learning. Journal of Computing and Electronic Information Management, 12(2), 105-108.
[16] Li, H., Zhang, Q., Zeng, M., Cao, J., Zhao, Q., & Hao, L. (2023). Insights into gas flow behavior in venturi aerator by CFD-PBM model and verification of its efficiency in sludge reduction through O3 aeration. Journal of Water Process Engineering, 54, 103960.
[17] Masarova, L., Verstovsek, S., Liu, T., Rao, S., Sajeev, G., Fillbrunn, M.,... & Signorovitch, J. (2024). Transfusion-related cost offsets and time burden in patients with myelofibrosis on momelotinib vs. danazol from MOMENTUM. Future Oncology, 1-12.
[18] Zhang, J., Zhao, Y., Chen, D., Tian, X., Zheng, H., & Zhu, W. (2024). MiLoRA: Efficient mixture of low-rank adaptation for large language models fine-tuning. arXiv. https://arxiv.org/abs/2410.18035
[19] Sun, Y., Pargoo, N. S., Ehsan, T., & Ortiz, Z. Z. J. (2024). VCHAR: Variance-Driven Complex Human Activity Recognition framework with Generative Representation. arXiv preprint arXiv:2407.03291.
[20] Liu, J., Li, K., Zhu, A., Hong, B., Zhao, P., Dai, S.,... & Su, H. (2024). Application of Deep Learning-Based Natural Language Processing in Multilingual Sentiment Analysis. Mediterranean Journal of Basic and Applied Sciences (MJBAS), 8(2), 243-260.
[21] Xu, Q., Feng, Z., Gong, C., Wu, X., Zhao, H., Ye, Z.,... & Wei, C. (2024). Applications of explainable AI in natural language processing. Global Academic Frontiers, 2(3), 51-64.
[22] Xu, T. (2024). Comparative Analysis of Machine Learning Algorithms for Consumer Credit Risk Assessment. Transactions on Computer Science and Intelligent Systems Research, 4, 60-67.
[23] Xu, T. (2024). Credit Risk Assessment Using a Combined Approach of Supervised and Unsupervised Learning. Journal of Computational Methods in Engineering Applications, 1-12.
[24] Xu, T. (2024). Fraud Detection in Credit Risk Assessment Using Supervised Learning Algorithms. Computer Life, 12(2), 30-36.
[25] Xu, T. (2024). Leveraging Blockchain Empowered Machine Learning Architectures for Advanced Financial Risk Mitigation and Anomaly Detection.
[26] Wang, J., Zhang, H., Zhong, Y., Liang, Y., Ji, R., & Cang, Y. (2024). Advanced Multimodal Deep Learning Architecture for Image-Text Matching. arXiv preprint arXiv:2406.15306.
[27] Wang, J., Li, X., Jin, Y., Zhong, Y., Zhang, K., & Zhou, C. (2024). Research on image recognition technology based on multimodal deep learning. arXiv preprint arXiv:2405.03091.
[28] Ahad, J., Ahmad, M., Farooq, A., Siddique, W., Waheed, K., Qureshi, K. R.,... & Irfan, N. (2023). Influence of throat and diverging section on the performance of venturi scrubber by using computational fluid dynamics. Progress in Nuclear Energy, 163, 104800.
[29] Xia, Y., Liu, S., Yu, Q., Deng, L., Zhang, Y., Su, H., & Zheng, K. (2023). Parameterized Decision-making with Multi-modal Perception for Autonomous Driving. arXiv preprint arXiv:2312.11935.
[30] Wambua, D. M. (2021). Environmental and Energy Requirements for Different Production Densities of Nile Tilapia (Oreochromis niloticus) in Recirculating Aquaculture Systems: Laboratory and Computer Simulation Studies (Doctoral dissertation, JKUAT-COETEC).
[31] Lin, Y. (2024). Application and Challenges of Computer Networks in Distance Education. Computing, Performance and Communication Systems, 8(1), 17-24.
[32] Lin, Y. (2024). Design of urban road fault detection system based on artificial neural network and deep learning. Frontiers in neuroscience, 18, 1369832.
[33] Lin, Y. (2024). Enhanced Detection of Anomalous Network Behavior in Cloud-Driven Big Data Systems Using Deep Learning Models. Journal of Theory and Practice of Engineering Science, 4(08), 1-11.
[34] Cheng, X., Xie, Y., Zhu, D., & Xie, J. (2019). Modeling re-oxygenation performance of fine-bubble–diffusing aeration system in aquaculture ponds. Aquaculture International, 27, 1353-1368.
[35] Xie, T., Li, T., Zhu, W., Han, W., & Zhao, Y. (2024). PEDRO: Parameter-Efficient Fine-tuning with Prompt DEpenDent Representation MOdification. arXiv preprint arXiv:2409.17834.